Eur J Nucl Med Mol Imaging (2011) 38 (Suppl 1):S41–S47
DOI 10.1007/s00259-011-1769-1

REVIEW ARTICLE

Three-dimensional radiobiological dosimetry (3D-RD) with ^{124}I PET for ^{131}I therapy of thyroid cancer

George Sgouros · Robert F. Hobbs · Francis B. Atkins · Douglas Van Nostrand · Paul W. Ladenson · Richard L. Wahl

Received: 11 January 2011 / Accepted: 22 February 2011 / Published online: 12 April 2011

Abstract Radioiodine therapy of thyroid cancer was the first and remains among the most successful radiopharmaceutical (RPT) treatments of cancer although its clinical use is based on imprecise dosimetry. The positron emitting radioiodine, ^{124}I, in combination with positron emission tomography (PET)/CT has made it possible to measure the spatial distribution of radioiodine in tumors and normal organs at high resolution and sensitivity. The CT component of PET/CT has made it simpler to match the activity distribution to the corresponding anatomy. These developments have facilitated patient-specific dosimetry (PSD), utilizing software packages such as three-dimensional radiobiological dosimetry (3D-RD), which can account for individual patient differences in pharmacokinetics and anatomy. We highlight specific examples of such calculations and discuss the potential impact of ^{124}I PET/CT on thyroid cancer therapy.

Keywords Three-dimensional radiobiological dosimetry · Radioiodine therapy · Thyroid cancer · Positron emission tomography

Supported by NIH NCI grant No. R01 CA116477.

G. Sgouros (✉) · R. F. Hobbs · R. L. Wahl
The Russell H. Morgan Department of Radiology,
Division of Nuclear Medicine, Johns Hopkins University,
School of Medicine,
Baltimore, MD, USA
e-mail: gsgouros@jhmi.edu

F. B. Atkins · D. Van Nostrand
Division of Nuclear Medicine, The Washington Hospital Center,
Washington, DC, USA

P. W. Ladenson
Department of Endocrinology, Johns Hopkins University,
School of Medicine,
Baltimore, MD, USA

Introduction

In chemotherapy-refractory and radiotherapy-ineligible patients, radiopharmaceutical (RPT) therapy offers viable treatment options where none exist. There are 114 active clinical trials for ^{131}I- and ^{90}Y-labeled agents, and 136 total trials (ClinicalTrials.gov), making RPT an area of ongoing clinical (and basic/translational) research. Dosimetry for RPT trials is based on 30- to 40-year-old standard geometry methods more appropriate for diagnostic than for therapeutic dosimetry. Response and toxicity prediction is essential to the rational implementation of cancer therapy. Unlike most other systemic treatments, the biological effects of radionuclide therapy are mediated via a well-defined physical quantity, the absorbed dose. The long and well-established cancer treatment experience in radiotherapy has provided ample evidence that absorbed dose may be used to predict biological response [1]. However, this experience has not translated into the routine incorporation of dosimetry-based treatment optimization in RPT. The prototypical example of this is also the oldest RPT—radioiodine treatment of thyroid cancer. The most recent American Thyroid Association (ATA) practice guidelines state that [2]:

> "Despite the apparent effectiveness of ^{131}I therapy in many patients, the optimal therapeutic activity remains uncertain and controversial [3].…Dosimetric methods are often reserved for patients with distant metastases or unusual situations such as renal insufficiency [4, 5] or when therapy with rhTSH stimulation is deemed necessary.…No prospective randomized trial to address the optimal therapeutic approach has been published.…In the future, the use of ^{123}I or ^{131}I with modern SPECT/CT or ^{124}I PET-based dosimetry may facilitate whole-body and

lesional dosimetry [6, 7]. In the treatment of locoregional or metastatic disease, no recommendation can be made about the superiority of one method of RAI administration over another (empiric high dose vs. blood and/or body dosimetry vs. lesional dosimetry.) Recommendation rating I."

Recommendation rating I is described as:

"Recommends neither for nor against. The panel concludes that the evidence is insufficient to recommend for or against providing the service or intervention because evidence is lacking that the service or intervention improves important health outcomes, the evidence is of poor quality, or the evidence is conflicting. As a result, the balance of benefits and harms cannot be determined."

Radioiodine treatment of metastatic differentiated thyroid cancer (DTC) is generally effective. In such a clinical scenario, reduced toxicity and improved survivor quality of life would be the main objectives of patient-specific dosimetry (PSD)-based treatment planning. The traditional approach to identifying the optimal dose of a new RPT, a controlled phase I RPT-based absorbed dose escalation trial, cannot be justified in thyroid cancer treatment. Rather, the accumulation, over time, of patient-specific absorbed dose calculations and tumor response or toxicity data will be required to identify the role of PSD in RPT therapy of metastatic thyroid cancer. The high-resolution, high-sensitivity data available from ^{124}I positron emission tomography (PET)/CT facilitates data collection for PSD calculations. In this report, case studies using the software package three-dimensional radiobiological dosimetry (3D-RD) with ^{124}I PET/CT in thyroid cancer are used to illustrate the kind of analysis that ^{124}I has enabled.

Three-dimensional radiobiological dosimetry (3D-RD)

Patient-specific, three-dimensional (3-D) image-based internal dosimetry involves using the patient's own anatomy and spatial distribution of radioactivity over time to obtain an absorbed dose calculation that provides as output the spatial distribution of absorbed dose. The results of such a patient-specific 3-D imaging-based calculation can be represented as a 3-D parametric image of absorbed dose, as dose-volume histograms over user-defined regions of interest or as the mean, and range of absorbed doses over such regions [8–15].

The earliest 3-D imaging-based targeted radionuclide dosimetry package, 3D-ID (three-dimensional internal dosimetry), described in the literature [16] was heavily influenced by treatment planning techniques developed for external radiotherapy treatment planning [17]. A next generation version of 3D-ID, named 3D-RD [18], has been developed that incorporates radiobiological modeling.

Radiobiological modeling was introduced by incorporating models derived from the linear-quadratic equation. The biologically effective dose (BED) which accounts for differences in dose rate [19] and the equivalent uniform dose (EUD) [20] which accounts for the impact of spatial distribution on response were incorporated. These models and their implementation for patient-specific dosimetry are described in detail elsewhere [18, 21–26]. To implement these models, absorbed dose rate images are calculated for each time point rather than the integrated absorbed dose from a cumulated activity map. This information, coupled with assignment of the radiobio-

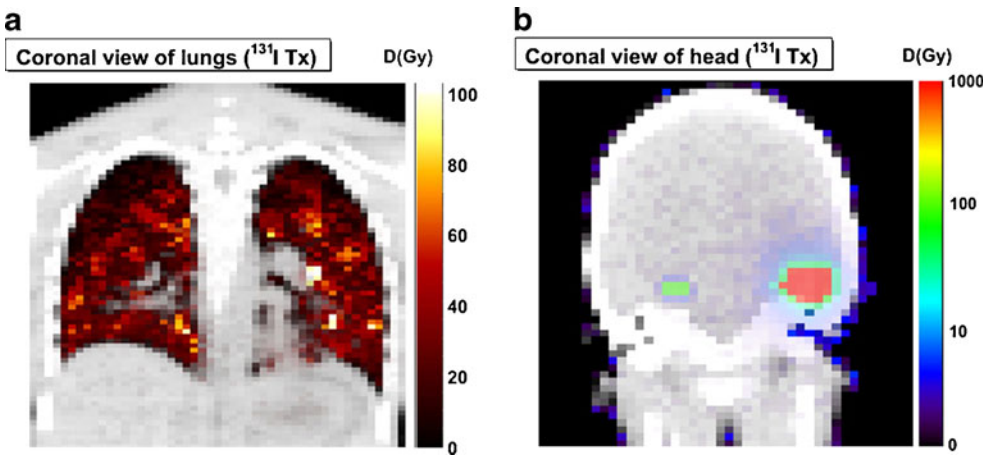

Fig. 1 Representative coronal slices of absorbed dose (*D*) maps of two different data sets: torso (measured) (**a**) and head (modeled) (**b**). In modeled calculation, average tumor activity concentration was placed in two tumor-associated volumes of interest defined using CT; voxels representing normal brain were assigned average (background) brain activity concentration. 3D-RD was then executed using these two as source regions of uniform activity irradiating normal brain. In this way, possible calculation artifacts associated with high tumor count–density gradients were avoided. Both images are viewed anteriorly

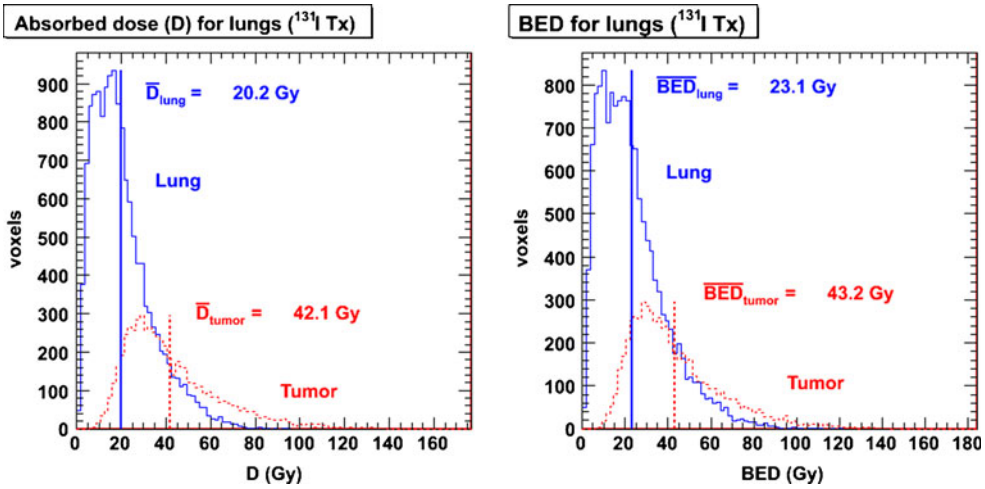

Fig. 2 Dose-volume histograms (and BED histograms) for the lung volume of interest voxels. The *blue histograms* represent normal lung tissue, while the *red lines* are tumor tissue. The *thick vertical lines* show the voxel averages

logical parameters, α, β, μ, the radiosensitivity per unit dose, radiosensitivity per unit dose squared, and the repair rate assuming an exponential repair process, respectively [22, 27], can be used to generate a BED value for each voxel, and subsequently an EUD value for a particular user-defined volume.

Real-time 3D-RD calculation and comparison with conventional dosimetry

A prospective or "real-time" implementation of an imaging-based Monte Carlo calculation using the 3D-RD dosimetry package [18] is illustrated for the radioiodine treatment of an 11-year-old girl, presenting post-thyroidectomy with metastatic papillary carcinoma [26]. The patient presented with radioiodine-avid bilateral temporal lobe lesions and diffuse lung metastases. Pulmonary function tests showed both obstructive and restrictive lung defects; the thyroglobulin concentration was 9,553 ng/ml. The real-time aspect of the 3D-RD calculations took advantage of the 3D-RD software package design that allows dose calculations to start without the need for the complete data set. This was accomplished by calculating the dose rate obtained from each scan at each time point and then integrating these over time after the last scan had been collected and processed. In this way, the time-intensive Monte Carlo calculations were performed during the interval between image acquisitions and the more rapid integration over time was performed on the dose rate images.

The disease-laden lungs were dose limiting in this case and treatment planning was designed to identify the administered activity that would deliver no more than 27 Gy to the entire lungs (including tumor). The administered activity corresponding to this limit was 5.11 GBq. Absorbed dose images and dose-volume histograms are shown in Figs. 1 and 2, respectively, for this activity level. Recognizing that most voxels are likely a combination of tumor and normal lung tissue due to the disseminated nature of the metastases [28], an effort was made to identify "tumor" vs "normal lung" voxels. Segmentation based on activity uptake at 24 h was applied; voxels with activity > 30 mBq/voxel were considered tumor, the rest normal lung tissue. Discrimination by density, determined by converting CT values, as used in a previous 3D-RD calculation [18], and clearance rate [29] did not provide as good and consistent a tumor delineation although there was a great degree of overlap between all the approaches considered. The voxel-averaged BED to lung voxels identified as tumor was 43.2 Gy. Accounting for the spatial nonuniformity of the absorbed dose to tumor gave an EUD of 23 Gy. The

Table 1 Dose value summary (Gy)

Tissue	Absorbed dose	BED	EUD
Lungs	2.98	2.99	-[a]
Kidneys	1.65	1.66	-
Liver	3.39	3.41	-
Spleen	0.98	0.99	-
T1	7.72	-[b]	2.98
T2	3.32	-	3.13
T3	110	-	16.8
T4	57.5	-	17.9
T5	101	-	20.2
T6	71.1	-	16.9
T7	13.6	-	6.54
T8	33.7	-	14.5
T9	25.2	-	11.8
T10	1.72	-	1.88
T11	61.5	-	28.4
T12	18.8	-	10.6
T13	12.2		7.05

[a] Not applicable to normal organs

[b] BED incorporated into EUD for tumors

BED values for the brain lesions were 1,220 and 142 Gy; the corresponding EUD values were 89.1 and 55.9 Gy.

The administered activity determined using OLINDA/EXM [30, 31] to deliver 27 Gy to the lungs was 3.14 GBq. Retrospective analysis revealed that the difference was due to the assumption of disease-free lungs and a reference lung mass in the OLINDA/EXM calculation. No lung mass assumption was needed in the 3D-RD calculation because the density as obtained from CT is applied to the calculation and this inherently accounts for target voxel mass. When the

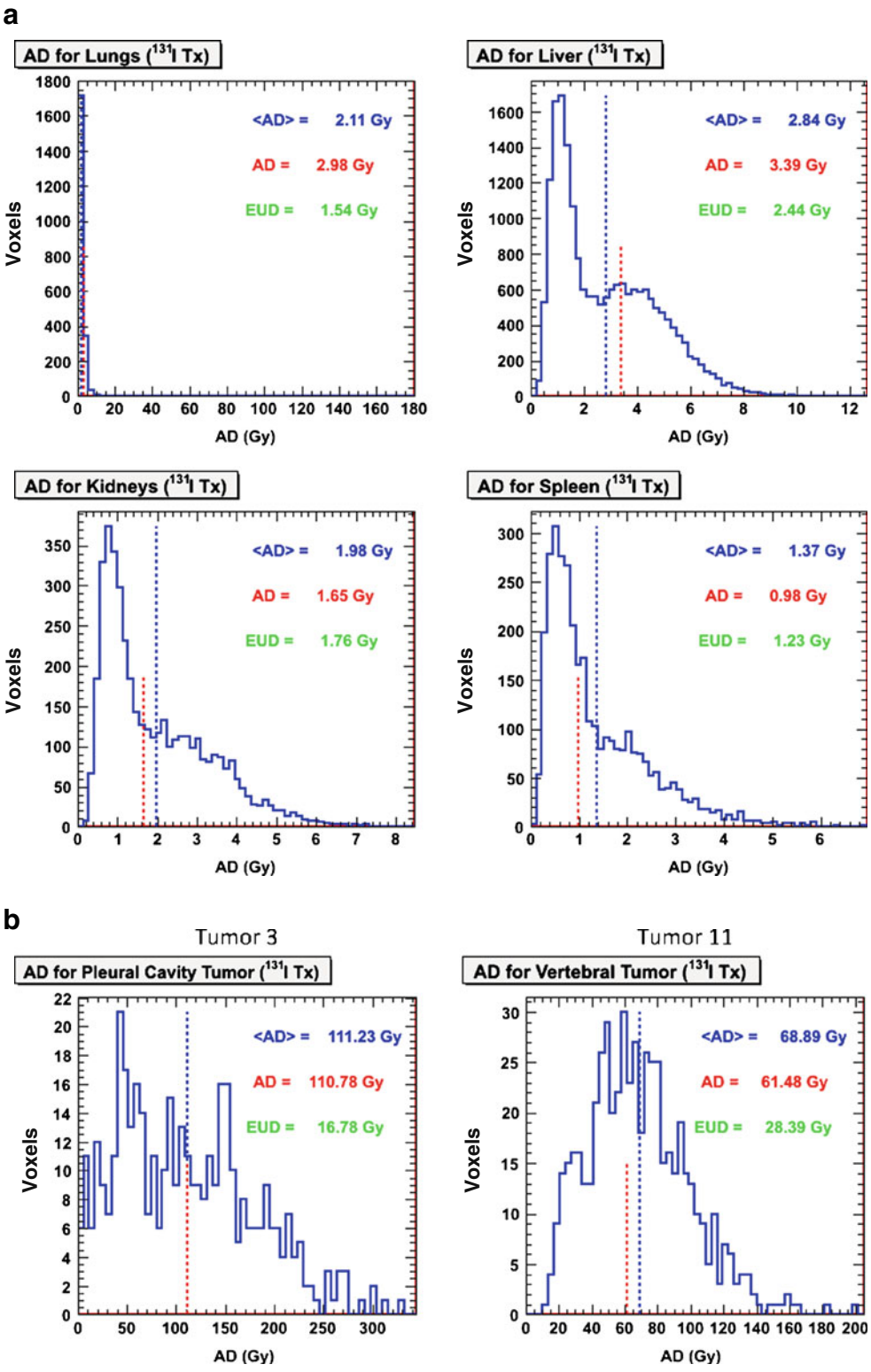

Fig. 3 **a** Dose-volume histograms (DVHs) for normal organs are shown with the voxel averaged absorbed dose (*blue dotted line*) and the mean absorbed dose obtained from a whole-organ contour (*red dotted line*) superimposed on the DVHs. **b** The DVH for two tumors receiving a mean absorbed dose of 110 Gy with an EUD of 16.8 Gy and a mean absorbed dose of 61.5 Gy with an EUD of 28.4 Gy. **c** Transverse and coronal cross sections depicting absorbed dose images of the two tumors in **b**

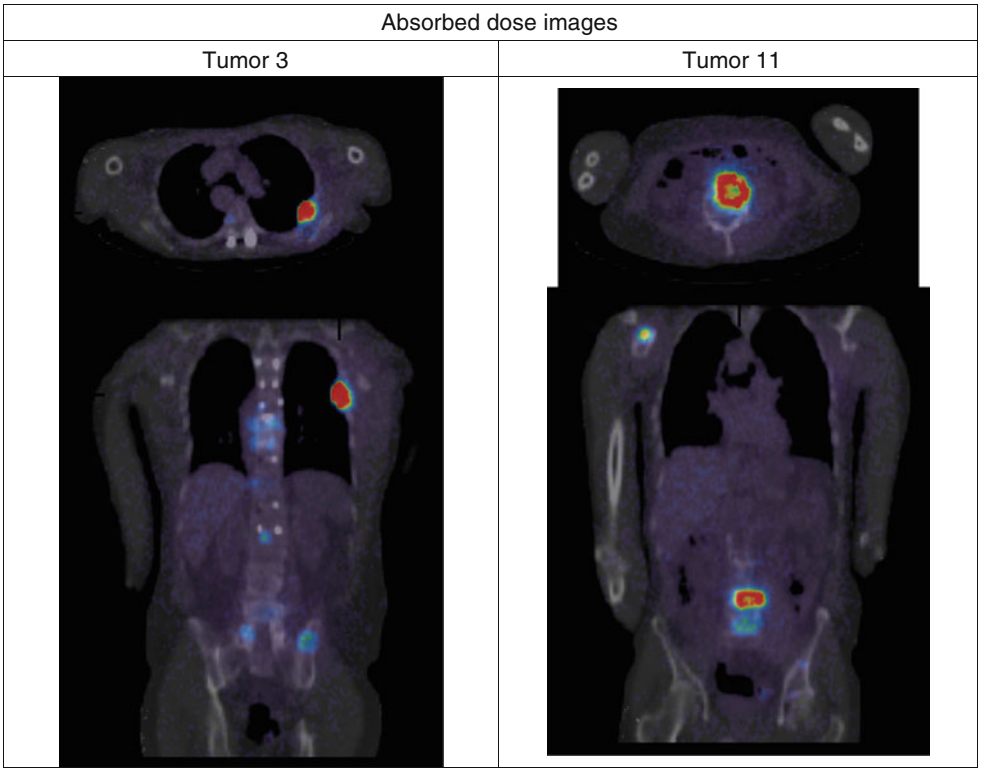

Fig. 3 (continued)

reference lung mass used in the OLINDA/EXM calculation was adjusted for the patient's total lung mass (as determined from the CT image using 3D-RD), an administered activity of 5.17 GBq was obtained.

The patient experienced no pulmonary, neurological, or other adverse clinical response to ^{131}I treatment. At 12 and 24 months of follow-up, the patient's serum thyroglobulin after comparable thyroid hormone withdrawal had declined from its pretreatment level, 9,553 ng/ml, to 777 and 130 ng/ml, respectively. The patient's left and right lobe metastatic lesions, which initially measured 24 and 9 mm, respectively, were both undetectable on cranial MRI at 26 months after initial radioiodine therapy.

Tumor dosimetry for retrospective evaluation of the EUD

As noted above, the EUD is a radiobiologically derived dosimetric parameter intended to reflect the impact of nonuniform tumor absorbed dose distributions on tumor control. We present another case study to illustrate the use of ^{124}I PET with 3D-RD in examining the role of EUD in thyroid cancer therapy.

Retrospective 3D-RD analysis was performed on a patient with metastatic DTC who initially presented with numbness in his right leg, and a tumor involving his thoracic spine identified on CT scan. Following emergency surgery the patient was treated with radioiodine. On 1-year follow-up, and with informed consent, a ^{124}I PET/CT imaging time course was collected following administration of 63 MBq (1.7 mCi) of ^{124}I. The patient was subsequently administered 3.7 GBq ^{131}I for therapy.

Results of the 3D-RD analysis are summarized in Table 1 and Fig. 3. Whole contour (as opposed to voxel averaged) mean absorbed doses were calculated for 13 tumors. The absorbed dose values ranged from 1.72 (tumor 10) to 110 Gy (tumor 3). The minimum and maximum EUD values were 1.88 (tumor 10) and 28.4 (tumor 11) Gy. The EUD values for the two tumors with the highest absorbed dose (110 and 101 Gy) are below the maximum EUD value found for tumor 11, which received an absorbed dose of 61.5 Gy. These results can be explained by examining the dose-volume histograms shown in Fig. 3b. The dose-volume histogram for tumor 11 has a relatively even distribution about the mean with no voxels receiving zero dose. This is in contrast to the dose-volume histograms for tumor 3, which show a large number of voxels with absorbed dose values below the mean, including voxels with a dose of zero.

Follow-up of this patient (and others from the same protocol) for tumor response evaluation is pending. The individual tumor response, measured as a change in tumor volume, will be compared with absorbed dose and EUD

values to determine if response better correlates with EUD as has been observed in lymphoma [32, 33]. Such studies provide a unique opportunity to evaluate radiobiological modeling for RPT in humans.

Conclusions

Real-time treatment planning using 3D-RD was demonstrated in a difficult pediatric thyroid case involving lung and brain metastases. Sequential ^{124}I PET/CT studies allowed dosimetry planning. A straightforward implementation of a simpler, alternative approach gave results substantially different from those obtained using 3D-RD. With appropriate corrections, however, the simpler alternative methodology gave values very similar to those obtained with 3D-RD; however, the needed corrections would not necessarily have been known without having performed the 3D-RD analysis for this patient. The 3D-RD analysis also provided more detailed information regarding potential efficacy and toxicity.

The second study illustrates how ^{124}I PET with 3D-RD can be used to validate radiobiological models in humans. Response follow-up of such patients will provide the critical data needed to evaluate the role of EUD and radiobiological modeling in predicting tumor response in metastatic DTC patients as a step towards a more rational approach to selecting the level of ^{131}I activity for therapy. SPECT-based lesion dosimetry analysis by Maxon et al. and Thomas et al. concluded that an 85- to 140-Gy mean tumor absorbed dose is needed for efficacy [34, 35]. The analysis provided in the second case study suggests that the EUD was likely substantially below the mean tumor absorbed dose in those studies and raises the possibility that mean tumor absorbed dose may not be the best predictor of tumor response.

It is not likely that ^{124}I PET/CT will be routinely performed for thyroid cancer treatment planning; rather analysis of a number of specific studies with this approach will help address the still unresolved question regarding the role of dosimetry in radioiodine treatment of thyroid cancer. Once resolved, ^{124}I PET/CT studies will remain valuable either in establishing an optimal SPECT/CT-based treatment planning methodology or in specific difficult cases that would benefit from the greater sensitivity, resolution, and quantitative accuracy of PET/CT ^{124}I imaging.

Conflicts of interest None.

References

1. Hellman S, Devita VT, Rosenberg SA. Principles of cancer management: radiation therapy. Cancer: principles & practice of oncology. 6th ed. Philadelphia: Lippincott Williams and Wilkins; 2001. p. 265–88.
2. American Thyroid Association (ATA) Guidelines Taskforce on Thyroid Nodules and Differentiated Thyroid Cancer, Cooper DS, Doherty GM, Haugen BR, Kloos RT, Lee SL, et al. Revised American Thyroid Association management guidelines for patients with thyroid nodules and differentiated thyroid cancer. Thyroid 2009;19(11):1167–214.
3. Van Nostrand D, Atkins F, Yeganeh F, Acio E, Bursaw R, Wartofsky L. Dosimetrically determined doses of radioiodine for the treatment of metastatic thyroid carcinoma. Thyroid 2002;12 (2):121–34.
4. Holst JP, Burman KD, Atkins F, Umans JG, Jonklaas J. Radioiodine therapy for thyroid cancer and hyperthyroidism in patients with end-stage renal disease on hemodialysis. Thyroid 2005;15 (12):1321–31.
5. Driedger AA, Quirk S, McDonald TJ, Ledger S, Gray D, Wall W, et al. A pragmatic protocol for I-131 rhTSH-stimulated ablation therapy in patients with renal failure. Clin Nucl Med 2006;31(8):454–7.
6. Sgouros G, Kolbert KS, Sheikh A, Pentlow KS, Mun EF, Barth A, et al. Patient-specific dosimetry for 131I thyroid cancer therapy using 124I PET and 3-dimensional-internal dosimetry (3D-ID) software. J Nucl Med 2004;45(8):1366–72.
7. Jentzen W, Hobbs RF, Stahl A, Knust J, Sgouros G, Bockisch A. Pre-therapeutic (124)I PET(/CT) dosimetry confirms low average absorbed doses per administered (131)I activity to the salivary glands in radioiodine therapy of differentiated thyroid cancer. Eur J Nucl Med Mol Imaging 2010;37(5):884–95.
8. Chiavassa S, Aubineau-Lanièce I, Bitar A, Lisbona A, Barbet J, Franck D, et al. Validation of a personalized dosimetric evaluation tool (Oedipe) for targeted radiotherapy based on the Monte Carlo MCNPX code. Phys Med Biol 2006;51(3):601–16.
9. Flux GD, Webb S, Ott RJ, Chittenden SJ, Thomas R. Three-dimensional dosimetry for intralesional radionuclide therapy using mathematical modeling and multimodality imaging. J Nucl Med 1997;38(7):1059–66.
10. Furhang EE, Chui CS, Kolbert KS, Larson SM, Sgouros G. Implementation of a Monte Carlo dosimetry method for patient-specific internal emitter therapy. Med Phys 1997;24(7):1163–72.
11. Kolbert KS, Sgouros G, Scott AM, Bronstein JE, Malane RA, Zhang J, et al. Implementation and evaluation of patient-specific three-dimensional internal dosimetry. J Nucl Med 1997;38 (2):301–8.
12. Behr TM, Sharkey RM, Sgouros G, Blumenthal RD, Dunn RM, Kolbert K, et al. Overcoming the nephrotoxicity of radiometal-labeled immunoconjugates: improved cancer therapy administered to a nude mouse model in relation to the internal radiation dosimetry. Cancer 1997;80(12 Suppl):2591–610.
13. Tagesson M, Ljungberg M, Strand SE. A Monte-Carlo program converting activity distributions to absorbed dose distributions in a radionuclide treatment planning system. Acta Oncol 1996;35 (3):367–72.
14. Sgouros G, Kolbert KS, Zaidi H. The three-dimensional internal dosimetry software package, 3D-ID. In: Therapeutic applications of Monte Carlo calculations in nuclear medicine. Philadelphia: Institute of Physics; 2002.
15. Kolbert KS, Pentlow KS, Pearson JR, Sheikh A, Finn RD, Humm JL, et al. Prediction of absorbed dose to normal organs in thyroid cancer patients treated with 131I by use of 124I PET and 3-dimensional internal dosimetry software. J Nucl Med 2007;48 (1):143–9.
16. Sgouros G, Barest G, Thekkumthala J, Chui C, Mohan R, Bigler RE, et al. Treatment planning for internal radionuclide therapy: three-dimensional dosimetry for nonuniformly distributed radionuclides. J Nucl Med 1990;31(11):1884–91.
17. Mohan R, Barest G, Brewster LJ, Chui CS, Kutcher GJ, Laughlin JS, et al. A comprehensive three-dimensional radiation treatment planning system. Int J Radiat Oncol Biol Phys 1988;15(2):481–95.

18. Prideaux AR, Song H, Hobbs RF, He B, Frey EC, Ladenson PW, et al. Three-dimensional radiobiologic dosimetry: application of radiobiologic modeling to patient-specific 3-dimensional imaging-based internal dosimetry. J Nucl Med 2007;48(6):1008–16.
19. Fowler JF. 21 years of biologically effective dose. Br J Radiol 2010;83(991):554–68.
20. O'Donoghue JA. Implications of nonuniform tumor doses for radioimmunotherapy. J Nucl Med 1999;40(8):1337–41.
21. Dale R. Use of the linear-quadratic radiobiological model for quantifying kidney response in targeted radiotherapy. Cancer Biother Radiopharm 2004;19(3):363–70.
22. Dale R, Carabe-Fernandez A. The radiobiology of conventional radiotherapy and its application to radionuclide therapy. Cancer Biother Radiopharm 2005;20(1):47–51.
23. Dale RG. The application of the linear-quadratic dose-effect equation to fractionated and protracted radiotherapy. Br J Radiol 1985;58(690):515–28.
24. Baechler S, Hobbs RF, Prideaux AR, Wahl RL, Sgouros G. Extension of the biological effective dose to the MIRD schema and possible implications in radionuclide therapy dosimetry. Med Phys 2008;35(3):1123–34.
25. Hobbs RF, Sgouros G. Calculation of the biological effective dose for piecewise defined dose-rate fits. Med Phys 2009;36(3):904–7.
26. Hobbs RF, Wahl RL, Lodge MA, Javadi MS, Cho SY, Chien DT, et al. 124I PET-based 3D-RD dosimetry for a pediatric thyroid cancer patient: real-time treatment planning and methodologic comparison. J Nucl Med 2009;50(11):1844–7.
27. Zaider M, Hanin L. Biologically-equivalent dose and long-term survival time in radiation treatments. Phys Med Biol 2007;52 (20):6355–62.
28. Freudenberg LS, Jentzen W, Müller SP, Bockisch A. Disseminated iodine-avid lung metastases in differentiated thyroid cancer: a challenge to 124I PET. Eur J Nucl Med Mol Imaging 2008;35 (3):502–8.
29. Kolbert KS, Hamacher KA, Jurcic JG, Scheinberg DA, Larson SM, Sgouros G. Parametric images of antibody pharmacokinetics in Bi213-HuM195 therapy of leukemia. J Nucl Med 2001;42 (1):27–32.
30. Stabin MG, Sparks RB. OLINDA: PC-based software for biokinetic analysis and internal dose calculations in nuclear medicine. J Nucl Med 2003;44(5):103P.
31. Stabin MG, Sparks RB, Crowe E. OLINDA/EXM: the second-generation personal computer software for internal dose assessment in nuclear medicine. J Nucl Med 2005;46(6):1023–7.
32. Amro H, Wilderman SJ, Dewaraja YK, Roberson PL. Methodology to incorporate biologically effective dose and equivalent uniform dose in patient-specific 3-dimensional dosimetry for non-Hodgkin lymphoma patients targeted with ^{131}I-tositumomab therapy. J Nucl Med 2010;51(4):654–9.
33. Dewaraja YK, Schipper MJ, Roberson PL, et al. ^{131}I-tositumomab radioimmunotherapy: initial tumor dose-response results using 3-dimensional dosimetry including radiobiologic modeling. J Nucl Med 2010;51(7):1155–62.
34. Maxon HR, Englaro EE, Thomas SR, Hertzberg VS, Hinnefeld JD, Chen LS, et al. Radioiodine-131 therapy for well-differentiated thyroid cancer—a quantitative radiation dosimetric approach: outcome and validation in 85 patients. J Nucl Med 1992;33(6):1132–6.
35. Thomas SR, Maxon HR, Kereiakes JG. In vivo quantitation of lesion radioactivity using external counting methods. Med Phys 1976;03(04):253–5.